PHYSICAL REVIEW B **79**, 224525 (2009)

Terahertz magnetotransport measurements in underdoped $Pr_{2-x}Ce_xCuO_4$ and comparison with angle-resolved photoemission

G. S. Jenkins,[1] D. C. Schmadel,[1] P. L. Bach,[1] R. L. Greene,[1] X. Béchamp-Laganière,[2] G. Roberge,[2] P. Fournier,[2] and H. D. Drew[1]

[1]*Department of Physics, Center for Nanophysics and Advanced Materials, University of Maryland, College Park, Maryland 20742, USA*

[2]*Département de Physique, Regroupement Québécois Sur Les Matériaux de Pointe, Université de Sherbrooke, Sherbrooke, Québec, Canada J1K 2R1*

(Received 4 March 2009; revised manuscript received 22 May 2009; published 22 June 2009)

We present magnetotransport measurements performed on underdoped $Pr_{2-x}Ce_xCuO_4$ at THz frequencies as a function of temperature and doping. A rapidly decreasing Hall mass is observed as the doping is reduced consistent with the formation of small electron Fermi pockets. However, both dc and infrared magnetotransport data strongly deviate from the predictions of transport theory within the relaxation-time approximation based on angular-resolved photoemission data. Furthermore, the Hall mass remains negative with no signature of a change in Fermi-surface topology at or above the Néel temperature and the characteristic temperature at which the optical gap fully closes. In the paramagnetic state, this behavior of the Hall mass may be qualitatively understood as arising from current vertex corrections to the Hall conductivity due to magnetic fluctuations as observed in overdoped $Pr_{2-x}Ce_xCuO_4$ [G. S. Jenkins *et al.*, arXiv:0901.1701 (unpublished)].

DOI: 10.1103/PhysRevB.79.224525 PACS number(s): 74.72.Jt, 78.20.Ls, 71.18.+y, 71.10.Ay

I. INTRODUCTION

The cuprates remain an intriguing problem because they are strongly interacting electron systems close to the Mott state characterized by strong competing fluctuations of charge, magnetic, and superconducting order. The subtle interplay between these fluctuations manifests as different behavior in the various cuprate versions.[1] Charge order is emphasized near 1/8 doping. Superconducting fluctuations extend to high temperatures in the hole-doped (*p*-type) cuprates. Magnetic order is more strongly expressed in the electron-doped (*n*-type) cuprates. Mott correlations as half filling is approached become particularly important in underdoped materials. The difficulty of describing the electronic properties of the cuprates may lie in the necessity to account for these different fluctuating orders simultaneously.

The predominance of magnetic order in the *n*-type cuprates has lead to the suggestion that they approach the Mott state through a spin-density-wave (SDW) transition at a quantum critical point near optimal doping. Evidence for this SDW order in the magnetic state is seen in the direct observation of a gap in angular-resolved photoemission (ARPES) measurements,[2] and an onset of gaplike optical absorption in the infrared whose frequency increases as half filling is approached.[1,3] No such gaplike feature is present in the *p*-type cuprates, which instead exhibit a suppression of spectral weight near the Fermi level at temperatures below a characteristic pseudogap temperature.[4] Both the gap and pseudogap produce Fermi arcs in ARPES measurements, wherein portions of the large holelike Fermi surface (FS) observed at optimal doping are obliterated.[5] In the case of *n*-type cuprates, the obliterated sections are reasonably hypothesized to result from a SDW gaping of the FS from the (π,π) magnetic order which doubles the unit cell and reconstructs the FS by zone folding, leading to a small electronlike Fermi pocket centered at $(\pi,0)$.[1]

In this paper, we examine the dc and infrared (IR) magnetotransport of underdoped *n*-type cuprates to test the SDW picture by comparing the transport data with ARPES data within conventional transport theory. In the magnetically ordered state with the absence of (π,π) magnetic fluctuations it might be expected that transport theory within the relaxation-time approximation (RTA) would be applicable. We have measured the Hall angle of four underdoped $Pr_{2-x}Ce_xCuO_4$ (PCCO) samples at an optical frequency of 10.5 meV. Our principle observation is large discrepancies between the magnetotransport data and the predictions of the RTA based on the Fermi-surface properties measured by ARPES.

II. MEASUREMENT AND RESULTS

Thin *c*-axis-oriented films of PCCO were grown via pulsed laser deposition onto $LaSrGaO_4$ (001) substrates. We report data on two samples which were previously measured in the near infrared[6] along with two new similarly grown samples.[7] The four samples have a chemical doping of $x=0.15$, 0.135, 0.12, and 0.10, thicknesses of 145, 220, 126, and 275 nm, and T_c's of 19.6, 12.5, and 2 K, and below the lowest measurable temperature of 2 K, respectively.

The Faraday rotation and circular dichroism characterized by the complex Faraday angle θ_F were measured at 10.5 meV as a continuous function of temperature. The output of a far-infrared molecular vapor laser was polarization modulated with a rotating quartz 1/4-wave plate and subsequently transmitted through the sample at normal incidence. Magnetic fields up to 8 T were applied parallel to the *c* axis of the film. The detector signal was harmonically analyzed and the complex Faraday angle extracted, a technique that is detailed elsewhere.[8]

In the thin-film limit, the complex Hall angle is derived from the Faraday angle via $\theta_H=(1+\frac{n+1}{Z_0\sigma_{xx}d})\theta_F$, where n is the index of refraction of the substrate, Z_0 is the impedance of free space, and d is the thickness of the film. The film thick-

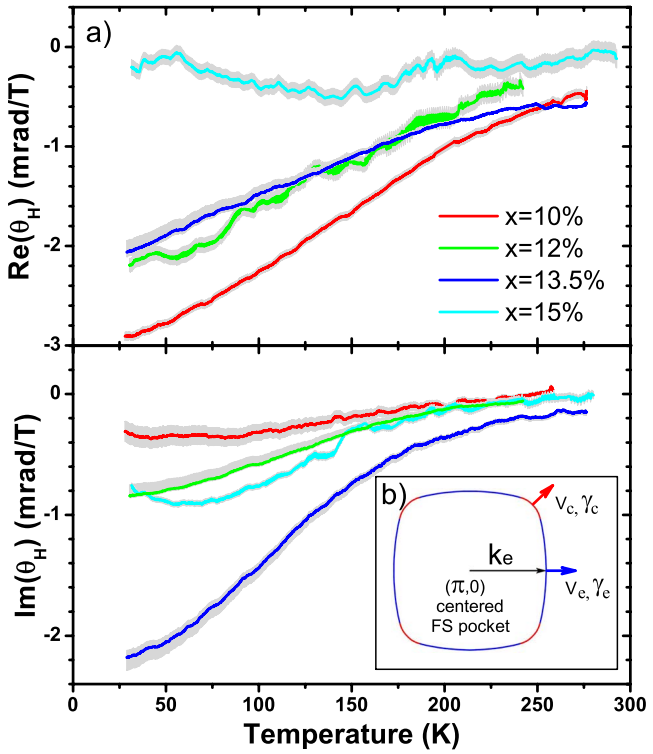

FIG. 1. (Color online) (a) Real and imaginary parts of the Hall angle measured at 10.5 meV as a function of temperature. A negative value implies a dominant electronlike response. Grey depicts an uncertainty of one standard deviation. (b) Schematic of the FS model of the electron pocket centered at $(\pi,0)$ as described in the text.

ness was chosen to allow sufficient transmitted power while maintaining a relatively small conversion factor. Fourier-transform infrared spectroscopic-transmission measurements were performed in the spectral range from 2 to 13 meV at a set of discrete temperatures ranging from 10 to 300 K. The complex conductivity was extracted by fitting the transmission data to a simple Drude model.[9]

The measured Hall angle as a function of temperature for all four samples is presented in Fig. 1(a). For all PCCO samples, the measured complex Faraday angle at fixed temperature was linear in applied field. The three lowest-doped samples exhibit a Hall response that is qualitatively consistent with a simple Drude model. Therefore, we parametrize the data in terms of a Drude model. The Hall frequency ω_H and Hall scattering rate γ_H are defined in terms of the complex Hall angle,

$$\theta_H = \frac{\sigma_{xy}}{\sigma_{xx}} = \frac{\omega_H}{(\gamma_H - i\omega)}, \tag{1}$$

where σ_{xy} is the Hall conductivity, σ_{xx} is the longitudinal conductivity, $\omega_H = qB/(m_H c)$ is the Hall frequency, ω is the radiation frequency, m_H is the effective Hall mass, B is the applied magnetic field, and q is the effective charge of the quasiparticle. The Hall mass can be expressed as

$$\frac{m_H}{m_e} = -\frac{\omega_c^e}{\omega}\mathrm{Im}(1/\theta_H), \tag{2}$$

where $\omega_c^e = 0.115$ meV/T is the bare electron cyclotron frequency and m_e is the bare electron mass.

Various calibrations of the IR Hall system were performed to ensure the accuracy and validity of the measurement technique.[8] A polarizer and wave plate substituted for the sample induce a rotation and ellipticity which are easily calculated and compared to measurements. To fully test the system under similar operating conditions as the measurements performed on high-T_c cuprates, a GaAs two-dimensional electron-gas (2DEG) heterostructure was measured as a function of magnetic field with a 25 $\Omega/\square$ thin film of NiCr deposited on the surface in order to lower the transmitted power to a level commensurate with a typical high-T_c sample. The cyclotron resonance of a 2DEG produces a resonance and antiresonance associated with the imaginary and real parts of the Faraday angle, respectively. Since the resonance and antiresonance are simply related, the relative sizes of the real and imaginary Faraday angles allow careful comparison with measurements. In addition, measurements performed on optimally doped single-crystal $Bi_2Sr_2CaCu_2O_{8+x}$ (BSCCO) measured at 10.5, 5.25, and 3.0 meV when analyzed with Eq. (2) demonstrate a temperature- and frequency-independent Hall mass[8] consistent with ARPES,[10] the optical mass derived from ac conductivity,[11] and the Hall mass derived from near-infrared Hall measurements.[12] The Hall masses extracted from the complex Hall-angle data for all PCCO samples are shown in Fig. 2.

III. COMPARISON OF LOW-TEMPERATURE IR HALL RESULTS AND ARPES

To test the simple SDW model, we compare dc and IR magnetotransport data directly with the reconstructed FS properties measured by ARPES. Both dc and IR Hall measurements are sensitive to Fermi-surface geometry as well as quasiparticle scattering rates and velocities, precisely the quantities measured by ARPES.

Generally in cuprate systems, it has been observed that ARPES measurements reflect the bulk band dispersion and FS topology. In overdoped PCCO in the $T \to 0$ limit, the measured dc R_H agrees with the value calculated from ARPES data in the RTA, and both are consistent with Luttinger's thereom.[14] In underdoped n-type cuprates, the number density of the electron pocket derived from ARPES measurements is consistent with the stoichiometric doping as measured in $Sm_{1.86}Ce_{0.14}CuO_4$ (Ref. 2) and optimally and underdoped $Nd_{2-x}Ce_xCuO_{4\pm\delta}$ (NCCO).[1,15,16] In optimally doped Bi-2212, the band dispersion as measured by the recent low-energy laser ARPES agrees with earlier higher-energy measurements verifying that both techniques are measuring bulk properties.[17] Calculated transport properties within the RTA (Ref. 18) derived from ARPES measurements on overdoped Tl-2201 (Ref. 19) agree with dc R_H, angle-dependent magnetoresistance,[20] and the FS area and cyclotron mass derived from de Haas–van Alphen measurements,[21] and all measurements agree with Lutting-

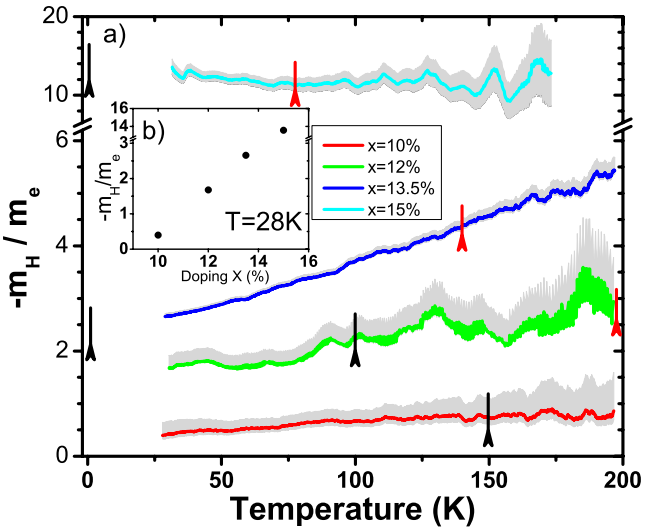

FIG. 2. (Color online) (a) The Hall mass is extracted from Fig. 1(a) using Eq. (2) and normalized to the bare electron mass. Temperatures above 200 K are excluded due to noise introduced into m_H from the exceedingly small Hall angle. The negative value of the Hall mass signifies a net electronlike response. The extremely small Hall masses associated with the 10% and 12% samples exemplify a large IR Hall response which cannot be obtained from ARPES data analyzed in terms of the RTA. The system fails to recover to a large holelike Fermi surface (positive m_H) well above the Néel temperature (marked by the lower temperature black arrows) (Ref. 13) as well as the characteristic temperature where the optical gap fully closes (marked by the higher temperature red arrows) (Ref. 3). (b) The low-temperature (28 K) Hall mass plotted versus doping.

er's thereom. Therefore, a careful comparison between ARPES and transport data is warranted.

Within the RTA in Boltzmann theory, the off-diagonal and diagonal conductivities (σ_{xy} and σ_{xx}) may be expressed as path integrals around the FS involving the Fermi velocity, scattering rate, and size and shape of the FS,[22]

$$\sigma_{xy} = \frac{e^2}{hc_0}\frac{e\vec{B}}{\hbar c}\oint_{\mathrm{FS}} dk \frac{\vec{v}_k^* \times d\vec{v}_k^*/dk}{(\gamma_k^* - i\omega)^2},$$

$$\sigma_{xx} = \frac{e^2}{hc_0}\oint_{\mathrm{FS}} dk \frac{|\vec{v}_k^*|}{\gamma_k^* - i\omega}, \tag{3}$$

where $\gamma_k^* = v_k^* \Delta k$, Δk is the momentum distribution curve (MDC) width as measured by ARPES, $l = 1/\Delta k$ is the mean-free path, v_k^* is the (renormalized) Fermi velocities measured by ARPES, and c_0 is the interplane spacing. In a comparison of ARPES and transport data, it is important to recognize that the current relaxation time that characterizes transport is not necessarily the same as the quasiparticle lifetime measured by ARPES. For example, small-angle elastic scattering as seen by ARPES does not affect transport.[22] Therefore, in implementing our model, we compare the γ^* needed to reproduce the transport data to the ARPES values.

As depicted in Fig. 1(b), we construct a two-arc FS model of the electron pocket centered at $(\pi,0)$ whose shape and size are based on ARPES. The blue and red arcs have different radii of curvature whose center defines the "edge" and "corner" of the pocket, respectively. The distance from the center of the pocket to the edge is k_e. The radius of curvature of the edge arc divided by k_e defines variable β_e. κ is the fraction of the FS which is made up of the edge arc lengths. Along with the condition that the tangent to the FS is continuous at all points, the three variables k_e, β_e, and κ define the size and shape of the FS. The corner and edge arcs are assigned ARPES measured values of Fermi velocities v_k^* and scattering rates γ_k^* computed from the MDC widths. Setting Fermi velocities and scattering rates along each arc to a constant is not strictly correct. However, if they are considered as effective average values along each arc then the model captures the quantitative features of the FS properties. Since the discrepancies between ARPES and transport data will be shown to be very large in comparison, errors which may be introduced into the analysis from this approximation are negligible. Utilizing Eq. (3), the complex IR Hall angle and dc Hall coefficient $R_H = \sigma_{xy}/\sigma_{xx}^2$ are calculated and compared to measurements. The results are presented in Table I.

Very little ARPES data actually exist for PCCO.[25] However, ARPES measurements have characterized various similar n-type cuprates at a variety of doping levels including $Nd_{2-x}Ce_xCuO_{4\pm\delta}$,[15,26,27] $Pr_{0.89}LaCe_{0.11}CuO_4$,[28] and $Sm_{1.86}Ce_{0.14}CuO_4$.[2] ARPES measurements together with dc-R_H data show fractionalization of a large holelike FS upon underdoping below a critical value ~16% into arcs gapped along the magnetic Brillouin zone (BZ).[1,2,15,24,29] Below a doping of ~13%, the arc in the vicinity of $(\pi/2, \pi/2)$ is completely gapped out[15] leaving only the arc near $(\pi,0)$. In this paper, we take the point of view that these observations correspond to the formation of a single convex electron pocket centered at $(\pi,0)$ in PCCO for $x<13\%$ and that the band-folded sections of FS are much reduced in intensity due to coherence factors in ARPES.[2]

The FS curvature associated with the edge sections of the electron pocket [defined in Fig. 1(b)] is an important consideration when calculating Hall transport. In the case of NCCO, the edge sections have a convex curvature at ~13%, become straight at around ~15%, and eventually become concave (or holelike) at ~16%.[15] Substitution of various lanthanide elements show a systematic correlation of edge section curvature with atomic number.[30] The edge sections become holelike at a crossover doping level which decreases with a decrease in lanthanide atomic number.[30] Based upon the measured trends, the curvature of the edge sections at ~12% of PCCO should be a bit flatter along the edge section than a sample of NCCO at the same doping. For PCCO, we expect a fully convex electron pocket with no holelike contributions at and below ~12% doping. Increasing the doping above ~13%, any holelike contributions caused from the edge curvature would be more prevalent in PCCO than NCCO.

From the published ARPES data,[2,15,16,25–28,30] reasonable values of the size and shape of the FS as well as the edge and corner Fermi velocities and scattering rates for excitation energies near the FS (below the observed kink in the energy dispersion) (Ref. 25) are summarized in Table I for 10% and 12% doping levels in rows 1 and 4, respectively. It should be noted that only one study reports the corner Fermi velocity,

TABLE I. Each row of the table represents a set of input parameters as measured by ARPES (in italics), fit parameters (underlined), and calculated results based on the RTA for R_H, IR Hall angle, and m_H normalized to measured values (in bold). ARPES measurements determine the size and shape of the FS represented by three parameters (k_e, β_e, and κ) as well as the related Fermi velocity and scattering rate parameters as depicted in Fig. 1(b) and defined in the text. Measured values of dc R_H at low temperature are -6.5×10^{-9} Ωm for the 10% sample (Ref. 23) and -6.2×10^{-9} Ωm for the 12% sample (Ref. 24). Using the measured ARPES parameters, strong deviations from dc and IR Hall experimental values are observed (rows 1 and 4). By fixing the Fermi velocities to those measured by ARPES and allowing the corner scattering rate γ_c to vary, a large mean-free path along the corner direction l_c is required to fit the dc-R_H data (rows 2 and 5). Simultaneously fitting the IR Hall and dc-R_H data requires a large v_c and $l_c\sim1.5l_e$ (rows 3 and 6), in contrast to the ARPES measured $l_c\sim0.4l_e$ and relatively small v_c, illustrating a fundamental breakdown of the relaxation-time approximation.

Doping	FS size and shape			FS properties				Mean-free path					
x (%)	k_e (1/Å)	β_e	κ	v_e (eV Å)	γ_e (eV)	v_c (eV Å)	γ_c (eV)	l_e (Å)	l_c (Å)	$\frac{R_H}{R_H^e}$	$\frac{\mathrm{Re}(\theta_H)}{\mathrm{Re}(\theta_H^e)}$	$\frac{\mathrm{Im}(\theta_H)}{\mathrm{Im}(\theta_H^e)}$	$\frac{m_H}{m_H^e}$
10	*0.207*	*2.50*	*0.75*	*1.5*	*0.06*	*0.6*	*0.06*	**25**	**10**	**0.4**	**0.3**	**0.5**	**5.6**
10	*0.207*	*2.50*	*0.75*	*1.5*	*0.06*	*0.6*	0.02	**25**	**36**	**1.0**	**0.5**	**4.2**	**8.2**
10	*0.207*	*2.50*	*0.75*	1.7	0.06	3.5	0.09	**27**	**40**	**1.0**	**1.0**	**1.0**	**1.0**
12	*0.221*	*7.50*	*0.65*	*1.5*	*0.06*	*0.6*	*0.06*	**25**	**10**	**0.2**	**0.2**	**0.1**	**2.7**
12	*0.221*	*7.50*	*0.65*	*1.5*	*0.06*	*0.6*	0.01	**25**	**41**	**1.0**	**0.7**	**2.0**	**2.3**
12	*0.221*	*7.50*	*0.65*	1.5	0.07	1.2	0.04	**21**	**35**	**1.0**	**1.0**	**1.0**	**1.0**

where $v_c\sim0.4v_e$,[2] but similar results have been obtained on $Nd_{1.85}Ce_{15}CuO_4$.[16] Below, we show the mean-free path and velocity associated with the corner arc required to fit the IR Hall and dc-R_H data within the RTA are many times larger than that estimated from ARPES measurements.

We focus on the two lowest-doped samples 10% and 12%, where no holelike contributions exist either from the hole pocket near $(\pi/2,\ \pi/2)$ observed at higher doping or from the concave curvature of the edge sections associated with the electron pocket. However, it should be emphasized that our fundamental observation is a very large Hall-angle response at low doping expressed as a small Hall mass. Admixtures of holelike contributions tend to reduce σ_{xy} which suppress the Hall response manifesting as a *large* apparent Hall mass. This enhancement of the apparent Hall mass is observed in the 15% sample, for example, see Figs. 1(a) and 2.

The number density calculated from the FS volume measured by ARPES is consistent with the stoichiometric doping to within 10%. However, the calculated dc R_H (Refs. 24 and 29) and the IR Hall data for the two lowest-doped samples are off significantly compared to the measured values (see Table I, rows 1 and 4). We emphasize that the discrepancy lies well outside of any measurement errors associated with input model parameters or transport values. To fully illustrate this large discrepancy, we consider two cases.

In the first case, we only consider the dc-R_H data. The Fermi velocities measured by ARPES are fixed but the scattering rate along the corner sections is allowed to vary in order to fit the dc R_H. The result that $l_c\sim1.5l_e$ (Table I, rows 2 and 5) is contrary to ARPES measurements reporting $l_c\lesssim(1/2)l_e$.[2]

A similar comparison between the low-temperature dc-R_H data and values calculated from a mean-field SDW model was performed by Lin and Millis.[1] They used a tight-binding band model with a doping-dependent SDW gap which produces a Fermi surface whose size and shape are very similar to that measured by ARPES. The Fermi velocities were weakly anisotropic such that $v_c/v_e\sim0.8$ compared with $v_c/v_e\sim0.4$ measured by ARPES. An isotropic scattering rate was assumed. Our model reproduces the same calculated Hall coefficient using the Fermi velocities calculated from their tight-binding model. The trend observed in their study that the measured dc R_H is significantly larger than expected becomes much more pronounced when the actual anisotropic velocities as measured by ARPES are used to calculate transport values.

Although the dc R_H can be fit by fixing the velocities measured by ARPES and adjusting only the corner scattering rates, the IR Hall data are off by over a factor of 2 and cannot be fit under any parameter values of the scattering rates assuming the ARPES measured Fermi velocities. Therefore, in the second case, we allow the Fermi velocities as well as scattering rates to vary to fit both the dc R_H as well as the low-temperature IR Hall data. The resulting values are significantly different from those measured by ARPES (Table I, rows 3 and 6). We still require $l_c\sim1.5l_e$ in order to fit the dc R_H as expected since dc R_H only depends upon the mean-free path, but to concurrently fit the IR Hall data requires a large v_c whereas ARPES measures a relatively small v_c.

This large discrepancy can be intuitively understood. For a simple one-band isotropic FS, $m_H\sim k_f/v_F$, so extremely small Hall masses result from strongly curved sections of FS (a small radius of curvature k_F, like at the corner sections of the electron pocket) and a large Fermi velocity. The more rigorous model shows this precise behavior requiring large velocities along the corner sections of FS (Table I, rows 3 and 6). The large discrepancy between the analyzed ARPES data and the dc and IR magnetotransport data elucidates a significant breakdown of the RTA approximation.

There are other observations which cast doubt on a simple SDW model fully describing the ground state in the underdoped n-type cuprates. The large increase in v_c required to describe the IR Hall data when doping from 12% to 10%

contradicts the mean-field SDW prediction. Using reasonable values in a tight-binding model (t, t', t'', and changes of the gap energy and Fermi energy with doping), a very gradual decrease in the velocities $\lesssim 25\%$ is expected as the doping is changed from 12% to 10%. However, in order to describe the IR Hall data, an increase in v_c by a factor of ~ 3 is required. Furthermore, the same tight-binding model predicts very little anisotropy of the Fermi velocity associated with the electron pocket such that $0.7 \lesssim v_c/v_e \lesssim 0.8$. However, the measured anisotropy by ARPES is a much larger factor $v_c/v_e \approx 0.4$. Note that to fit the IR Hall data tabulated in Table I (rows 3 and 6) requires anisotropies in velocity in the opposite sense, $v_c/v_e \approx 2$ for the 10% sample. Lastly, ARPES data show a weak remnant large unreconstructed holelike FS superimposed upon the reconstructed FS suggesting that a simple SDW may not capture all the physics associated with the underdoped state.[2] However, it should be noted that this effect would tend to suppress the Hall-angle response due to the admixture of holelike contributions reducing σ_{xy}, a trend which is contrary to the observed large dc and IR Hall response.

In this section, we have shown that the low-temperature dc-R_H response associated with the 10% and 12% doped samples is anomalously large compared to that expected from ARPES measurements. Our measured IR Hall-angle response was also shown to be anomalously large characterized by a small and doping-dependent Hall mass. These deviations were shown to lie well outside the error bars associated with any of the measurements. The discrepancy between ARPES and magnetotransport measurements signals a breakdown of the RTA.

IV. TEMPERATURE DEPENDENCE OF THE HALL MASS

In Fig. 2(a), the three lowest-doped samples show a gradual increase in Hall-mass parameter with temperature. A similar behavior is observed in the dc R_H (Refs. 23, 24, and 29) and dc $\cot(\theta_H)$ (Ref. 31) for similarly underdoped samples in which the response is electronlike at low temperature and gradually decreases in magnitude with increasing temperature. This behavior is qualitatively consistent with a rollover from a small electronlike FS below the Néel temperature to a large holelike FS in the paramagnetic state at high temperatures. In this scenario, the Hall angle would be expected to be negative at low temperatures eventually becoming positive, crossing zero in the interim. At the zero crossing, the apparent Hall frequency would be zero and the corresponding Hall-mass parameter would be infinite. In a simple SDW scenario, the switch over from the large and negative Hall mass and Hall coefficient to the values corresponding to the large Fermi surface would be expected above the Néel temperature. The Néel temperature for the n-type cuprates is relatively low as depicted in Fig. 2(a): $T_N|_{10\%} \approx 150$ K, $T_N|_{12\%} \approx 100$ K, $T_N|_{13.5\%} \approx 0$, and $T_N|_{15\%} \approx 0$.[13] Furthermore, the IR optical gap which fully closes at a temperature T_W has been measured as a function of doping and is represented in Fig. 2(a): $T_W|_{10\%} \approx 280$ K, $T_W|_{12\%} \approx 200$ K, $T_W|_{13.5\%} \approx 140$ K, and $T_W|_{15\%} \approx 80$ K.[3] It is therefore very surprising that the Hall masses and Hall coefficients maintain a negative electronlike response and only change gradually through and above T_N and T_W.

These observations in the paramagnetic state of underdoped PCCO are similar to the observations in overdoped PCCO, where there is no long-range order and only the large holelike Fermi surface is observed by ARPES. In this case, the negative m_H and R_H have been shown to arise from current vertex corrections to σ_{xy} arising from (π, π) magnetic fluctuations in the paramagnetic state.[14] The current vertex corrections were shown to successfully describe the salient features of the dc and IR Hall-angle measurements as a function of temperature, doping, and frequency.[14] Therefore, we expect this mechanism to also apply to the paramagnetic state of underdoped PCCO. The full recovery of the large holelike FS is expected only well above the Néel temperature, where antiferromagnetic (AFM) fluctuations are negligible. In this interpretation, the absence of an anomaly at the Néel temperature is caused by a continuous evolution from the paramagnetic state where current vertex corrections are active to the magnetically ordered phase where the Fermi surface reconstructs at the Néel temperature. How this paramagnetic state influenced by magnetic fluctuations above T_N evolves smoothly into a magnetically ordered state below T_N is an important question that needs further study.

V. DISCUSSION

In this section, we discuss possible origins of the observed discrepancies of the dc and IR magnetotransport data with ARPES data analyzed within the RTA. First, we note that the discrepancy associated with the dc R_H is not explained by Mott correlations since R_H is not affected by the quasiparticle spectral weight.[32] This suggests that vertex corrections to the conductivity are the relevant effect. Vertex corrections arising from AFM fluctuations in the paramagnetic state account for the anomalous dc and IR magnetotransport in overdoped PCCO.[14,33,34]

Further insight into the nature of the ac magnetotransport can be obtained from the following expression for the Hall mass:

$$\frac{m_H}{m_e} = -\frac{\omega_c^e}{\omega}\frac{|\sigma_{xx}|}{|\sigma_{xy}|}\sin(\phi_H - \phi_C), \tag{4}$$

where $\sigma_{xx} = |\sigma_{xx}|e^{i\phi_C}$, $\sigma_{xy} = -|\sigma_{xy}|e^{i\phi_H}$, and $\omega_c^e = 0.115$ meV/T is the bare electron cyclotron frequency.

From Eq. (4), it can be seen that a reduced m_H can occur in two ways. First, $|\sigma_{xx}|$ can reduce more rapidly than $|\sigma_{xy}|$. This is the expectation for small pockets as σ_{xx} is proportional to the Fermi circumference and σ_{xy} tends to be less dependent on the size of the Fermi pocket [see Eq. (3)]. Note that a mixture of holelike and electronlike contributions to σ_{xy} leads to a reduction in $|\sigma_{xy}|$ and a corresponding *increase* in m_H. Alternatively, a strong reduction in m_H can occur due to a diminishing phase difference. Moreover, to achieve a zero crossing of m_H as suggested by the data in Fig. 2(b) below a doping of $\sim 9\%$, it is necessary to have a sign change in $\phi_H - \phi_C$.

Therefore, the observed rapid reduction in m_H may signal a reduction in ϕ_H relative to ϕ_C which may provide an im-

portant clue to the nature of the corresponding interactions causing deviations from the RTA predictions. Some insight into this possibility is gained by expressing the conductivity in an extended Drude parameterization. We can write to lowest order in ω/Γ,

$$\phi_H \cong \frac{2\omega(1+\lambda_H)}{\Gamma_H}, \quad \phi_C \cong \frac{\omega(1+\lambda_C)}{\Gamma_C}, \tag{5}$$

where $\Gamma_H(\lambda_H)$ and $\Gamma_C(\lambda_C)$ are the relaxation rates (mass enhancement parameters) for σ_{xy} and σ_{xx} respectively. From Eqs. (4) and (5), it is seen that a reduced λ_H with a nearly constant Γ_H will lead to a reduced m_H. The $\lambda_H/\lambda_C<1$ behavior is expected based on frequency dependent IR Hall studies of BSCCO and $YBa_2Cu_3O_{6+x}$ (YBCO).[35,36] These effects can arise from vertex corrections.[33–35]

In underdoped PCCO, the vertex corrections from magnetic fluctuations should be significantly modified from those observed in overdoped PCCO due to the long-range magnetic order.[14] That is, below the Néel temperature, AFM fluctuations are absent so that vertex corrections would need to arise from some other interaction effect. Apart from phonons, the possibilities are charge and magnons.

In the magnetically ordered phase the magnon excitations near the center of the magnetic BZ can mediate the electron-electron interaction in the small electron pocket. The strong electron-magnon interaction in the cuprates implies that these interactions can affect the electron transport. However, the discrepancies of the experimental data with the RTA mean that vertex corrections are needed to explain the data in terms of the electron-magnon interaction.

The observed temperature dependence of R_H and m_H supports this scenario as discussed in the previous section. Moreover, the absence of a magnetotransport signature of the Néel temperature indicates a continuous transition from the magnetic fluctuation-induced conserved vector current (CVC) in the paramagnetic phase to magnon-induced CVC in the antiferromagnetic phase.

Charge fluctuations related to stripe order can also lead to vertex corrections. The nearly square electron Fermi surfaces observed in ARPES implies nesting associated with the nearly flat edges. This nesting could lead either to a charge-density-wave ground state with long-range charge order or vertex corrections to the conductivity due to charge-order fluctuations. These two possibilities produce similar effects, namely, a reduction in the low-frequency contributions to σ_{xx} from some of the edge segments of the FS. A reduction in σ_{xx} implies an enhancement of R_H and θ_H (and therefore a suppression in m_H). However, CDW ordering would be expected to reconstruct the electron pocket leading to nearly one-dimensional segments of FS with some holelike curvature induced by the CDW gap, thus, reducing σ_{xy} as well. Furthermore, the electron pocket associated with the 12% sample is more square than that of the 10% sample. Any CDW effects observed in transport measurements should be more pronounced in the 12% pocket, although the Hall mass continues to dramatically decrease with underdoping. We believe that these arguments make the CDW scenario unlikely, although a more thorough theoretical examination of the mixed SDW and CDW effects on the transport is necessary.

VI. CONCLUSION

We measured the IR Hall angle as a function of temperature and doping at an excitation energy of 10.5 meV. Although the data are qualitatively consistent with the formation of a small electron pocket in underdoped PCCO, neither the dc-R_H data nor IR Hall-angle response at low doping is consistent with ARPES data when analyzed under the assumptions of the relaxation-time approximation. The large discrepancy between transport and ARPES data demonstrates a clear breakdown of the RTA implying the importance of including vertex corrections in the conductivity. A negative and continuously increasing Hall mass well above the Néel temperature observed in all underdoped samples is difficult to explain within a SDW model in the ordered phase but may be understood in terms of current vertex corrections from AFM fluctuations in the paramagnetic state, similar to the case of the overdoped PCCO.[14]

ACKNOWLEDGMENTS

The authors wish to acknowledge the support of NSERC, FQRNT, CFI, CNAM, and NSF (Contracts No. DMR-0653535 and No. DMR-0303112). We wish to thank N. P. Armitage, M. Ikeda, V. Galitski, H. Kontani, T. D. Stanescu, Changyoung Kim, and T. Takahashi for insightful discussions. We thank S. Pelletier and K. D. Truong for their technical assistance.

[1] J. Lin and A. J. Millis, Phys. Rev. B **72**, 214506 (2005).
[2] S. R. Park, Y. S. Roh, Y. K. Yoon, C. S. Leem, J. H. Kim, B. J. Kim, H. Koh, H. Eisaki, N. P. Armitage, and C. Kim, Phys. Rev. B **75**, 060501(R) (2007).
[3] A. Zimmers, J. M. Tomczak, R. P. S. M. Lobo, N. Bontemps, C. P. Hill, M. C. Barr, Y. Dagan, R. L. Greene, A. J. Millis, and C. C. Homes, Europhys. Lett. **70**, 225 (2005).
[4] T. Timusk and B. Statt, Rep. Prog. Phys. **62**, 61 (1999).
[5] A. Damascelli, Z. Hussain, and Z.-X. Shen, Rev. Mod. Phys. **75**, 473 (2003).
[6] A. Zimmers, L. Shi, D. C. Schmadel, W. M. Fisher, R. L. Greene, H. D. Drew, M. Houseknecht, G. Acbas, M.-H. Kim, M.-H. Yang, J. Cerne, J. Lin, and A. Millis, Phys. Rev. B **76**, 064515 (2007).
[7] G. Roberge, S. Charpentier, S. Godin-Proulx, K. D. Truong, P. Fournier, and P. Rauwel, J. Cryst. Growth (to be published).
[8] G. S. Jenkins, Ph.D. thesis, University of Maryland at College Park, 2003.
[9] A. Kuzmenko, REFFIT program v1.2.54.
[10] T. Valla, A. V. Fedorov, P. D. Johnson, Q. Li, G. D. Gu, and N. Koshizuka, Phys. Rev. Lett. **85**, 828 (2000).
[11] J. J. Tu, C. C. Homes, G. D. Gu, D. N. Basov, and M. Strongin,

Phys. Rev. B **66**, 144514 (2002).
[12] D. C. Schmadel, Ph.D. thesis, University of Maryland at College Park, 2002.
[13] E. M. Motoyama, G. Yu, I. M. Vishik, O. P. Vajk, P. K. Mang, and M. Greven, Nature (London) **445**, 186 (2007).
[14] G. S. Jenkins, D. C. Schmadel, P. L. Bach, R. L. Greene, X. Bechamp-Laganiere, G. Roberge, P. Fournier, H. Kontani, and H. D. Drew, arXiv:0901.1701 (unpublished).
[15] H. Matsui, T. Takahashi, T. Sato, K. Terashima, H. Ding, T. Uefuji, and K. Yamada, Phys. Rev. B **75**, 224514 (2007).
[16] N. P. Armitage and S. R. Park, and Changyoung Kim (private communication).
[17] J. D. Koralek *et al.*, Phys. Rev. Lett. **96**, 017005 (2006).
[18] G. S. Jenkins, D. C. Schmadel, A. B. Sushkov, G. D. Gu, H. Kontani, and H. D. Drew (unpublished).
[19] M. Platé *et al.*, Phys. Rev. Lett. **95**, 077001 (2005).
[20] D. C. Peets, J. D. F. Mottershead, B. Wu, I. S. Elfimov, R. Liang, W. N. Hardy, D. A. Bonn, M. Raudsepp, N. J. C. Ingle, and A. Damascelli, New J. Phys. **9**, 28 (2007).
[21] B. Vignolle, A. Carrington, R. A. Cooper, M. M. J. French, A. P. Mackenzie, C. Jaudet, D. V. C. Proust, and N. E. Hussey, Nature (London) **455**, 952 (2008).
[22] A. J. Millis and H. D. Drew, Phys. Rev. B **67**, 214517 (2003).
[23] Y. Onose, Y. Taguchi, K. Ishizaka, and Y. Tokura, Phys. Rev. Lett. **87**, 217001 (2001).
[24] Y. Dagan, M. M. Qazilbash, C. P. Hill, V. N. Kulkarni, and R. L. Greene, Phys. Rev. Lett. **92**, 167001 (2004).
[25] P. Richard, M. Neupane, Y.-M. Xu, P. Fournier, S. Li, P. Dai, Z. Wang, and H. Ding, Phys. Rev. Lett. **99**, 157002 (2007).
[26] N. P. Armitage *et al.*, Phys. Rev. Lett. **88**, 257001 (2002).
[27] F. Schmitt, W. S. Lee, D.-H. Lu, W. Meevasana, E. Motoyama, M. Greven, and Z.-X. Shen, Phys. Rev. B **78**, 100505(R) (2008).
[28] H. Matsui, K. Terashima, T. Sato, T. Takahashi, M. Fujita, and K. Yamada, Phys. Rev. Lett. **95**, 017003 (2005).
[29] P. Fournier (unpublished).
[30] M. Ikeda, T. Yoshida, A. Fujimori, M. Kubota, K. Ono, H. Das, T. Sahadasgupta, K. Unozawa, Y. Kaga, T. Sasagawa, and H. Takagi, arXiv:0803.4059 (unpublished).
[31] Y. Dagan and R. L. Greene, Phys. Rev. B **76**, 024506 (2007).
[32] T. D. Stanescu, V. Galitski, and H. D. Drew, Phys. Rev. Lett. **101**, 066405 (2008).
[33] H. Kontani, J. Phys. Soc. Jpn. **75**, 013703 (2006).
[34] H. Kontani, Rep. Prog. Phys. **71**, 026501 (2008).
[35] D. C. Schmadel, G. S. Jenkins, J. J. Tu, G. D. Gu, H. Kontani, and H. D. Drew, Phys. Rev. B **75**, 140506(R) (2007).
[36] In mid-IR Hall measurements, a reduced Γ_H compared with Γ_C is observed. By Kramers-Kronig relations, this implies that $\lambda_H/\lambda_C < 1$ in the far-IR spectral region.